THEORETICAL INVESTIGATION AND ANALYSIS OF TIME RESPONSE IN HETEROSTRUCTURE GEIGER-APD

ТЕОРЕТИЧЕСКОЕ ИССЛЕДОВАНИЕ И АНАЛИЗ ВРЕМЕННОГО ОТКЛИКА В ГЕТЕРОСТРУКТУРЕ APD-ГЕЙГЕР

© 2012 г.   **Mehdi Dehghan**

Department of Electrical Engineering, Firoozabad Branch, Meymand Center, Islamic Azad University, Meymand, Iran

E-mail: m_dehghan592@yahoo.com

In this paper the mean current impulse response and standard deviation in Geiger mode for heterostructure APD are determined. The model is based on recurrence equations. These equations are solved numerically to calculate the mean current impulse response and standard deviation as a function of time. In this structure we illustrate the multiplication region with different ionization threshold energies that the impact ionization of the injected carrier type is localized and the feedback carrier type is suppressed. In fact for this structure, better control of spatial distribution of impact ionization for both injected and feedback carriers can be achieved. By enhancing the control of impact-ionization position, the structure achieved to high gain and very low noise.

1. Introduction

Avalanche photodiodes (APDs) are famously known as detectors in long-haul fiber optic systems and Geiger mode applications due to their advantage of high internal gain generated by avalanche multiplication [1]. According to the local-field avalanche theory, both the multiplication noise and the gain-bandwidth product of APDs are determined by the ratio of the electron and hole ionization coefficients of the semiconductor in the multiplication region. Since this ratio is a material property, for a given electric field, efforts to improve the APD performance have focused on optimizing the electric field profile and characterizing new materials. A great deal of research has been devoted to reducing the multiplication noise of APDs by suppressing the feedback process and making the impact-ionization process itself more deterministic [2].

Recently, lower multiplication noise and higher gain-bandwidth products have been achieved by submicrometer scaling of the thickness of the multiplication region. The heterostructure APD (HAPD) was first proposed by Chin et al [3] to minimize the excess noise factor. An electron or hole may gain extra energy when cross over a band-edge discontinuity which would enhance the impact ionization. Proper selection of the heterojunction material layer will determine the degree of enhancement in ionization coefficient. However, Chia *et al* [4] found that no enhancement of ionization coefficients was observed in $Al_xGa_{1-x}As/GaAs$ HAPDs. Their measurements suggested that the excess energy gained by the carriers crossing the heterojunction interface is negligible. Later, it has been proved by Kwon et al [5] that low noise could be achieved in HAPDs when the finite initial energy of carriers entering the multiplication region.

Above breakdown the APD operates in the Geiger mode, so that a single absorbed photon can generate a measurable current APDs used as single photon detectors are referred to as single photon avalanche diodes (SPADs). Groves et al [6] showed how to calculate the mean current
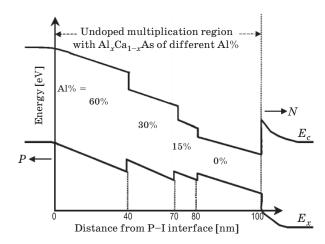
Fig. 1. Band structure of multiplication region in the I^2E structure.

impulse response and standard deviation in PIN APD structure for Geiger mode. In this letter we generalize the technique of Groves to show mean current and standard deviation of impact ionization engineered (I^2E) structure in Geiger mode. Band structure is shown in Fig. 1. The multiplication region consisted of a 40 nm thick $Al_{0.6}Ga_{0.4}As$ followed by 30 nm $Al_{0.3}Ga_{0.7}As$, 10 nm $Al_{0.15}Ga_{0.85}As$ and 20 nm GaAs.

The paper is organized as follows. In Section 2, the modified model to calculate the mean current impulse response and standard deviation by solving the recurrence equations is presented. In section 3, we demonstrate the results for I^2E structure. Finally we close this paper by conclusion, in section 4.

2. Theory of Model

We consider an APD with a multiplication region of width w. A parent photo-electron is injected into the multiplication region at $x = 0$

with a fixed velocity v_e under the effect of an electric field. After traveling a fixed dead space d_e, in the x-direction, the electron becomes capable of impact ionizing with an ionization coefficient α. Upon ionization, an electron-hole pair is generated, so that the parent electron is replaced by two electrons and a hole. The hole travels in the $(-x)$-direction and becomes capable of impact ionizing with an impact ionization coefficient β only after traveling a dead space d_h. This avalanche of ionization events continues until all carriers exit the multiplication region. In the case of multiplication with a fixed dead space d_e, the probability density function (pdf) of carriers vs time τ and distance ξ is given by

$$h_e(\xi, \tau) = \begin{cases} 0 & \xi \le d_e \\ \alpha \exp[-\alpha(\xi - d_e)]\delta(\tau - \xi/v_e) & \xi > d_e \end{cases}, \quad (1)$$

$$h_h(\xi, \tau) = \begin{cases} 0 & \xi \le d_h \\ \beta \exp[-\beta(\xi - d_h)]\delta(\tau - \xi/v_h) & \xi > d_h \end{cases}, \quad (2)$$

where d_e and d_h are the electron and hole dead spaces, respectively; v_e and v_h are the velocity of the electrons and holes, respectively; α and β are the ionization rates for electrons and holes, respectively, that often modeled by standard equation [7, 8] –

$$\alpha(E), \beta(E) = A \exp\left(-\left(\frac{E_c}{E}\right)^m\right). \quad (3)$$

Here A, E_c and m are the parameters taken from [9]. With integration of this distribution function over the total time, the position dependent ionization pdf is given as

$$h_{e(h)}(\xi) = \int_0^\infty h_{e(h)}(\xi, \tau)d\tau. \quad (4)$$

The recurrence equation for electron and hole mean current impulse response are given by [10]

$$\left\langle I_e(z, t)\right\rangle = P_e(z, t)\left\langle I_e(z, t)\right\rangle +$$
$$\int_0^{\min(w-z, v_e t)}\left(2\left\langle I_e(z+\xi, t-\xi/v_e)\right\rangle + \left\langle I_h(z+\xi, t-\xi/v_e)\right\rangle\right)h_e(\xi)d\xi, \quad (5)$$

$$\left\langle I_h(z, t)\right\rangle = P_h(z, t)\left\langle I_h(z, t)\right\rangle +$$
$$\int_0^{\min(w-z, v_h t)}\left(2\left\langle I_h(z+\xi, t-\xi/v_h)\right\rangle + \left\langle I_e(z+\xi, t-\xi/v_h)\right\rangle\right)h_h(\xi)d\xi, \quad (6)$$

where the first terms on the right-hand side of these equations represent the contributions from the injected, primary currents $\langle I_{e(h)0}(z, t)\rangle$.

The probabilities that the injected carriers avoid ionizing before exiting the multiplication region before time t is given by

$$P_e(z,t) = 1 - \int_0^{\min(w-z,\, v_e t)} h_e(\xi)\, d\xi, \qquad (7)$$

$$P_h(z,t) = 1 - \int_0^{\min(z,\, v_h t)} h_h(\xi)\, d\xi. \qquad (8)$$

The initial current from electrons and holes can be calculated as

$$I_{e0}(z,t) = \begin{cases} 0 & t > (w-z)/v_e \\ q v_e / w & t \le (w-z)/v_e \end{cases}, \qquad (9)$$

$$I_{h0}(z,t) = \begin{cases} 0 & t > (w-z)/v_e \\ q v_h / w & t \le (w-z)/v_e \end{cases}. \qquad (10)$$

The standard deviation of the impulse response can be determined by developing the recurrent expressions for the second order statistics of $I_e(z,t)$, $I_h(z,t)$ using the same technique used for the mean currents. The second moment of the impulse response $i_2(z,t) = \langle I^2(z,t) \rangle$ can be computed by

$$\langle I_e^2(z,t) \rangle = P_e(z,t) \langle I_{e0}^2(z,t) \rangle + \int_0^{w-z} d\zeta \int_0^t \Big[2\langle I_e^2(z+\zeta, t-\tau) \rangle + 2\langle I_e(z+\zeta, t-\tau) \rangle^2 + \qquad (11)$$
$$\langle I_h^2(z+\zeta, t-\tau) \rangle + 4\langle I_h(z+\zeta, t-\tau) \rangle \times \langle I_e(z+\zeta, t-\tau) \rangle \Big] \times h_e(\zeta, \tau)\, d\tau,$$

$$\langle I_h^2(z,t) \rangle = P_h(z,t) \langle I_{h0}^2(z,t) \rangle + \int_0^{z} d\zeta \int_0^t \Big[2\langle I_h^2(z+\zeta, t-\tau) \rangle + 2\langle I_h(z+\zeta, t-\tau) \rangle^2 + \qquad (12)$$
$$\langle I_e^2(z+\zeta, t-\tau) \rangle + 4\langle I_h(z+\zeta, t-\tau) \rangle \times \langle I_e(z+\zeta, t-\tau) \rangle \Big] \times h_h(\zeta, \tau)\, d\tau.$$

And the standard deviation of $I(z,t)$ can then be obtained using [11]

$$\sigma(z,t) = \sqrt{i_2(z,t) - i^2(z,t)}. \qquad (13)$$

The dark current is defined by [12] as

$$I_d = \frac{\theta_1 A \bar{X} V_{Bias} \left(\bar{X} V_{Bias} + V_{BI} \right)}{w_m} \times \\ \times \exp\left(-\frac{\theta_2 w_m}{\bar{X} V_{Bias} + V_{BI}} \right) + \frac{\bar{X} V_{Bias}}{R_d}, \qquad (14)$$

where

$$\theta_1 = \frac{\sqrt{2 m_c / E_g}}{h^2} q^3, \quad \theta_2 = \frac{2\gamma m_c^{0.5} E_g^{1.5}}{q h}, \\ \bar{X} = \frac{X}{X+1}, \qquad (15)$$

R_d is the parasitic leakage resistance, m is the effective mass of electron, γ is the constant depending on the shape of the tunneling barrier, h is the Planck's constant, and E_g is the energy gap.

3. Results and Discussion

Figure 2 shows the mean current impulse response to pure electron injection for I^2E avalanche photodiode which normalized to the injected primary current $q v_e / w$, as a function

of normalized time $t v_e / w_t$, where w_t is the total thickness of multiplication region ($w_t = 100$ nm). We assume equal ionization parameters for electrons and holes, take $d_e = d_h = 0.5$ nm, $v_e = v_h = 10^5$ m/s.

By contrast, in Geiger mode the standard deviation grows with an exponential rate twice that of the mean current impulse response, so that the standard deviation grows with the same exponential growth rate as its mean current impulse response. With having of standard deviation we can found the behavior of excess
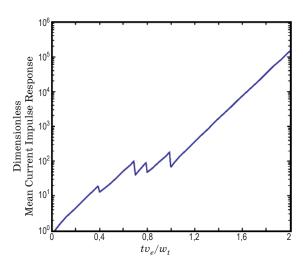
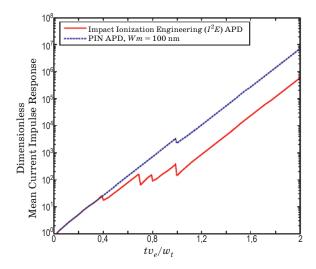**Fig. 2.** Mean current impulse response for I^2E structure.

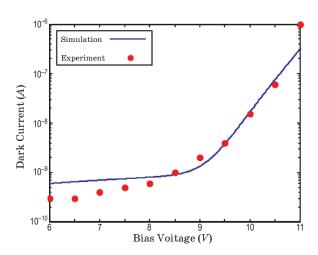**Fig. 3.** Comparison of dimensionless standard deviation in PIN and I^2E structure.

Fig. 4. Experimental and calculated dark current as a function of bias voltage at $T =$ $= 300$ K.

Fig. 5. Comparison of dark current in PIN-APD and I^2E structure at $T = 300$ K.

Fig. 6. Periodic voltage pulse used in Geiger mode.

noise in this structure. In Fig. 3 we compare the standard deviation in I^2E structure and $Al_{0.6}Ga_{0.4}As$ homojunction with $w = 100$ nm, $d_e = d_h = 0.5$ nm, $v_e = v_h = 10^5$ m/s, $k = 1$. According to this figure we can found that the $Al_{0.6}Ga_{0.4}As$ homojunction exhibits the highest standard deviation and ultimately highest excess noise compared to I^2E structure.

Experimental and calculated dark current for I^2E structure as a function of applied bias at $T = 300$ K are shown in Fig. 4 [13]. From the calculations, we can see that the breakdown voltage for this structure is 11.5 V. For low bias, the dark current is dominated by diffusion
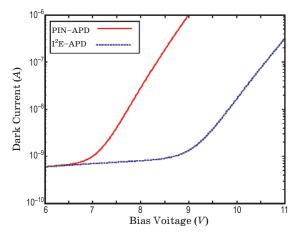
current and parasitic leakage current, and for higher bias, the tunneling current plays an important role. As seen from this figure, the calculated results are in agreement with the measured results.

Figure 5 shows comparison of dark current in PIN-APD and I^2E structure at $T = 300$ K. According to this figure, low dark current was achieved in I^2E structure.

We use of the 4V periodic voltage pulse as shown in Fig. 6, for bias APD above the breakdown in Geiger mode.

Breakdown voltage for this APD is 11.5 V. Figure 7 shows dark count rate as a function of over voltage for I^2E structure at T = 300 K. From this figure we can see that with increase of over voltage, the dark count rate is increased.

A separate absorption and multiplication (SAM) $Al_{0.6}Ga_{0.4}As/GaAs$ avalanche photodiode with I^2E structure in the multiplication region was shown in Fig. 8. The low noise characteristics associated with the initial-energy effect can be
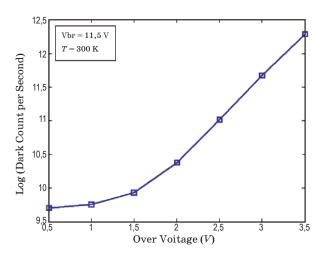
Fig. 7. Dark count as a function of over voltage at $T = 300$ K for I^2E structure.

Fig. 9. Dependence of the standard deviation in $Al_{0.6}Ga_{0.4}As/GaAs$ heterostructure APDs on the width of the $Al_{0.6}Ga_{0.4}As$ energy-build up layer.
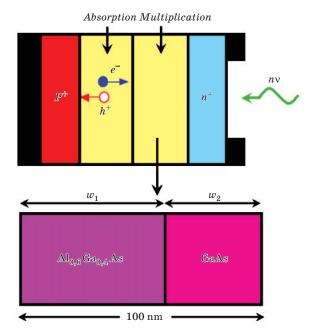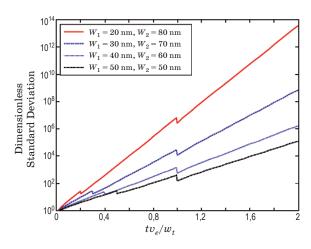

Fig. 8. Separate Absorption and Multiplication APD with I^2E structure in the multiplication region.

achieved by utilizing a two-layer multiplication region. A high bandgap $Al_{0.6}Ga_{0.4}As$ material, termed the energy-buildup layer (w_1), is used to elevate the energy of injected carriers without incurring significant multiplication events, while a second GaAs layer (w_2) with lower bandgap energy is used as the primary carrier multiplication layer.

In the calculations, the standard deviation is computed for different widths of the $Al_{0.6}Ga_{0.4}As$ layer while the total multiplication layer width was fixed at 100 nm. The results are shown in Fig. 9. The figure shows that with increase of energy-buildup layer thickness (w_1) the standard deviation and ultimately the excess noise factor are increased.

4. Conclusions

In this paper, we used recurrence equation to investigation of mean current impulse response and standard deviation for I^2E structure with four and two layer heterostructure multiplication regions in the Geiger mode. By enhancing the control of the impact ionization position, we achieved to low noise for these structures. We anticipate that this approach can be incorporated into separate absorption and multiplication structures and extended to long-wavelength materials for optical communication applications.

* * * * *

REFERENCES

1. *Tan C.H., David J.P.R., Plimmer S.A., Rees G.J., Tozer R.C., Grey R.* // IEEE Trans. Electron Devices. 2001. V. 48. P. 1310–1317.

2. *Groves C., Chia C.K., Tozer R.C., David J.P.R., Rees G.J.* // IEEE J. Quantum Electron. 2005. V. 41. P. 70−75.

3. *Chin R., Holonyak N., Stillman G.E., Tang J.Y., Hess K.* // Electron. Lett. 1980. V. 16. P. 467−469.

4. *Chia C.K., Ng B.K., David J.P.R., Rees G.J., Tozer R.C., Hopkinson M., Airey R.J., Robson P.N.* // J. Appl. Phys. 2003. V. 94. P. 2631−2637.

5. *Kown O.* // IEEE J. Quantum Electron. 2003. V. 39. P. 1287−1296.

6. *Groves C., Tan C.H., David J.P.R., Ress G.J., Hayat M.M.* // IEEE Trans. Electron Devices. 2005. V. 52. P. 1527−1534.

7. *Moll J.L., Meyer N.* Solid State Electron. 1961. V. 3. P. 155−161.

8. *Saleh M.A., Hayat M.M., Saleh B.E.A., Teich M.C.* IEEE Trans. Electron Devices. 2000. V. 47. P. 625−633.

9. *Plimmer S.A., David J.P.R., Grey R., Rees G.J.* IEEE Trans. Electron Devices. 2000. V. 47. P. 1089−1097.

10. *Tan C.H., Hambleton P.J., David J.P.R., Tozer R.C., Rees G.J., Lightwave J.* Technol. 2003. V. 21. P. 155−159.

11. *Hayat M.M., Saleh B.E.A., Lightwave J.* Technol. 1992. V. 10. P. 1415−1425.

12. *Chen W., Liu Sh.* IEEE Journal of Quantum Electronics. 1996. V. 32. 2105−2111.

13. *Wang S., Sidhu R., Zheng X.G., Li X., Sun X., Holmes A.L., Jr., Campbell J.C.* IEEE Photon. Technol. Lett. 2001. V. 13. P. 1341−1348.